Research Project Technical Completion Report
Project A-014-Ida

Spring Evapotranspiration from Low Sagebrush Range in Southern Idaho

Project Investigator *G. H. Belt*

Water Resources Research Institute
University of Idaho
Moscow, Idaho
October, 1970

Research Project Technical Completion Report
Project A-014-IDA
July 1, 1968- June 30, 1969

Spring Evapotranspiration from Low Sagebrush Range in Southern Idaho

by
G. H. Belt
Associate Professor
College of Forestry, Wildlife and Range Science
University of Idaho
Moscow, Idaho

This study has been a cooperative endeavor supported financially by the following organizations:

Office of Water Resources Research, Department of Interior, through Water Resources Research Institute, University of Idaho, Moscow, Idaho.

Forest, Wildlife and Range Experiment Station, University of Idaho, Moscow, Idaho.

Soil and Water Conservation Research Division, Northwest Branch, A.R.S., Department of Agriculture, Boise, Idaho.

Manuscript Prepared February, 1970
for Administrative Use Only

CONTENTS

LIST OF TABLES

PAGE

LIST OF FIGURES

APPENDIX

Spring Evapotranspiration from Low Sagebrush Range in Southern Idaho

I. INTRODUCTION

Approximately 75-85 percent of the 8-20" of average annual precipitation on southern Idaho rangelands is delivered in the form of winter snow and spring rain. During spring and summer months the annual charge of soil moisture necessary for forage production is depleted by the process of evapotranspiration, E.T. This report summarizes E.T. estimates made on the Reynolds Creek Experimental Watershed, Reynolds, Idaho, during May and June 1969.[1] These estimates were based upon measurements of meteorological parameters and evaluation of the energy balance.

Objectives

Objectives of the study were twofold:

1. To measure the magnitude of and variation in evaporative flux rates for low sagebrush range.
2. To identify those parameters of the microclimate which were significant in causing daily and hourly variation in flux rates.

Site Description

The Sheep Creek site is situated at an elevation of 5,400 feet on an open ridge. Plant species present are low

---

[1]The author greatfully acknowledges cooperation and support of ranchers in the Reynolds area who provided access to their lands and to the personnel of the Northwest Branch, Soil and Water Conservation Research Division, who rendered invaluable assistance in the collection and processing of data.

sagebrush, Artemisia arbuscula (38 percent crown cover) and Sandberg bluegrass, Poa secunda (2 percent). Average height of the vegetation was 17.0 cm. The soil is a Serala stony, gravelly loam with appreciable surface gravel. The site is typical of a large portion of the Reynolds Creek drainage.

Weather

During the spring measurement periods, frontal weather moving into the area resulted in partly cloudy or overcast conditions and subsequent reduction in the average daily flux of net radiation. Air temperatures ranged from 16 to 30 degrees centigrade. Vapor pressure ranged from 9 to 12 mb while total atmospheric pressure ranged from 24.5 to 24.8 mb. Wind velocity at 3.3m ranged from 0.8 to5.0 m/sec.

Soil Moisture

Soil moisture profiles were measured twice during the observation period. Both gravimetric surface measurements (upper 1" of soil) and neutron-probe, subsurface measurements (at 1, 2, 3, 4, 5, and 6 foot intervals) were made. The surface moisture ranged from 7 to 15 percent (dry weight) and was quite variable as a result of shower activity associated with the frontal weather. With soil moisture ranging from 17-40 percent by volume, subsurface measurements indicated a loss from the upper 3 feet and a gain in moisture in the lower 3 feet as shown in Table 1. These measurements were combined with precipitation measurements (0.34") and an

estimated soil moisture loss from the upper 6" of soil of -0.42". Assuming no surface flow, this suggests for the period May 29 to June 9 a total storage change of 0.80". This is interpreted as an average E.T. rate of 0.066" per day.

Table 1. Soil moisture measurements in inches determined with neutron probe Sheep Creek Study site.

	Profile Depth (ft.)					
Date	0.5-1.5	1.5-2.5	2.5-3.5	3.5-4.5	4.5-5.5	5.5-6.5
5/29/69	2.80	4.45	4.55	4.43	4.56	4.56
6/9/69	1.97	4.45	4.53	4.32	4.77	4.59
Storage	-.83	0	-.02	-.11	+.21	+.03

II. METHODS

Energy Balance - Bowen Ratio Technique

Evapotranspiration was estimated by analysis of the energy balance of the study site. The Bowen ratio was used to separate energy not partitioned into net radiation or soil heat flux, into either sensible or latent heat. Details of these methods are available in the literature (1) as are critical reviews of the methodology (2, 3).

Briefly, the method is derived from consideration of the heat energy budget given by:

$$R_n + G + H + LE = 0 \qquad (1)$$

where

R_n = net radiation incident on the surface

G = soil heat flux

H = sensible heat flux

LE = latent heat flux

The quantities R_n and G are measured directly with instruments. Since $-(R_n + G) = H + LE$, the magnitude of H + LE is known. The problem is to separate H from LE.

This is done after the method of Bowen(4) by recognition of the fact that the Bowen ration, H/LE, can be expressed as:

$$\frac{H}{LE} = \beta = \frac{C_p \rho K_H \, d\bar{\theta}/dz}{L K_Q \rho \, d\bar{q}/dz} \qquad (2)$$

where

C_p is the specific heat of air at constant pressure

(0.24), ρ is the density of air, θ is potential temperature, Q is specific humidity, K_H and K_Q are coefficients of eddy diffusivity for heat and water vapor respectively, L is the latent heat of vaporization and Z is height above the surface.

Assuming K_H equal to K_Q permits simplification of equation (2) to:

$$\frac{H}{L\overline{E}} = \beta = \frac{C_p \, d\overline{\theta}}{L \, d\overline{Q}} \qquad (3)$$

(The bar above $\overline{Q}$ and $\overline{\theta}$ denotes averaged quantities.) Averaging in this study was done over a 30 min. period.

Since Q can be expressed in terms of vapor pressure, e, and total atmospheric pressure, P, by:

$$Q = \frac{0.622e}{P} \qquad (4)$$

equation three can be expressed in finite terms as:

$$\beta = \frac{0.24 \; (837.1)}{586 \; (0.622)} \frac{\Delta\overline{\theta}}{\Delta\overline{e}} = 0.551 \frac{\Delta\overline{\theta}}{\Delta\overline{e}} \qquad (5)$$

Total atmospheric pressure P remained relatively constant at 24.7 in hg or 837.1 mb. The latent heat of vaporation was taken to be a constant 586 cal/cc at 20 C.

With measurements of the mean potential temperature gradient $\Delta\overline{\theta}$ and the mean vapor pressure gradient $\Delta\overline{e}$, β can be deduced from equation 5. Using β, equation 1 can be solved for LE as:

$$LE = \frac{-(R_n + G)}{\beta + 1} \qquad (6)$$

In this study, E.T. rates were determined by evaluation of equations 5 and 6 using values averaged over a thirty

minute period.

Measurements

Measurements were made with an automated measuring and recording system which logged meteorological parameters and coded paper tape suitable for computer entry. A schematic diagram of the recording system is given in figure 1. A description of instruments used, errors involved and sampling periods is given in Table 2. Instruments used in this study are commonly known with the exception of the Cambridge dew-point hygrometer, the shop built sampling system and integrated circuit counters. The counters, used with the anemometer system, are discussed in the Appendix.

The hygrometer is a "primary standard" instrument providing continuous measurement of dewpoint temperature. An air stream passing through the sensor is cooled by a mirror-like surface until moisture forms on the surface.

A servo system controls the temperature of the mirror and maintains it "just at" the dewpoint temperature. A platinum resistance thermometer imbedded in the mirror surface, registers the dewpoint temperature. Error in the dewpoint determination, approximately $\pm$0.2 C between successive readings or $\pm$0.4 C absolute are described in detail in Note 992N2 available from the manufacturer.[2] In the range of vapor pressures encountered in this study, this permitted

[2]Manufacturer is Cambridge Systems, Inc., 50 Hunt Street, Newton, Massachusetts.

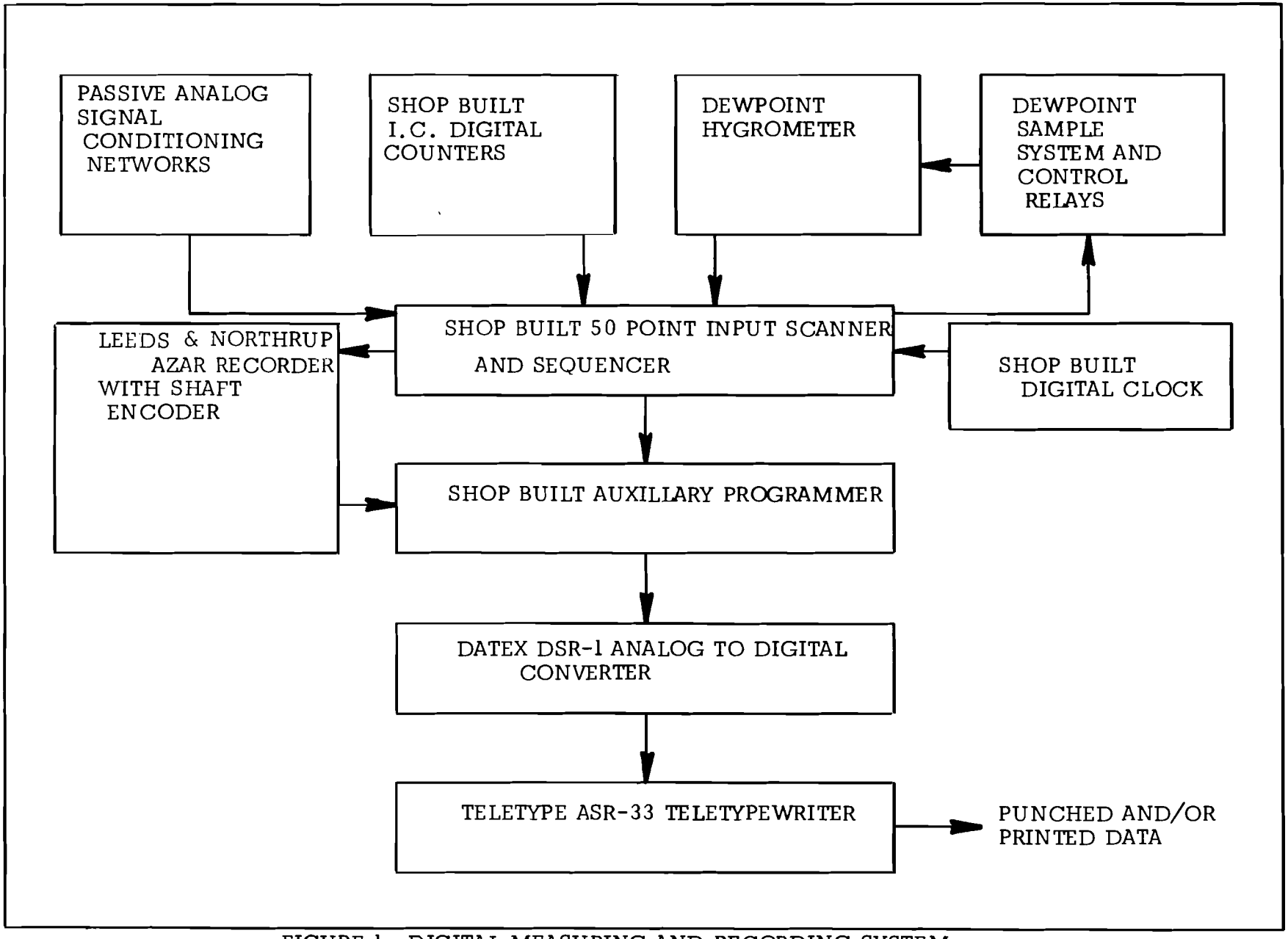

FIGURE 1: DIGITAL MEASURING AND RECORDING SYSTEM

Table 2: Instrumentation & Sampling

Measurement & Units	Measurement Error	No. of Inst.	Frequency of Measuring Each Inst/3 min.	Type of Instrument
Wind Velocity (cm/sec)	± 2.5 cm/sec	6	1	Thornthwaite cup anemometers
Air temperature °C	± .1° C	6	1	Shielded, aspirated 3-junction copper-constantan thermopile with 150°C reference junction
Incoming Solar Radiation Ly/min	± .02 Ly/min	1	1	Kipp & Zonen Solarimeter
Reflected Solar Radiation Ly/min	± .02 Ly/min	1	1	Kipp & Zonen Solarimeter
Net Radiation Ly/min	± .02 Ly/min	2	1	C.S.I.R.O. "FUNK" net radiometer & Fritschen, miniature net radiometer
Soil Heat Flux Ly/min	± .05 Ly/min	3	1	C.S.I.R.O. Soil heat flux plates
Vapor Pressure mb.	± .2 mb @ 10 mb	1	1	Cambridge systems model 992-C1 Dewpoint hygrometer combined with shop built air sample system. Sample system permits dewpoint determination at each of two levels every six minutes.
Wind Direction Degrees	± 5°	1	1	Shop made, Voltage divider

measurement within $\pm$0.2mb.

The shop built sampling system is shown schematically in Figure 2.

A and B are steel cylinders with a volume of approximately 4 liters. The cylinders were exhausted by the Millipore vacuum pump at such a rate that air within the tanks was exchanged every 2.5 minutes. The air flow rate was adjusted by use of a Dwyer control valve. Air sample intake hoses, 1 and 2, were made of 1/4" Impolene tubing and were 150 feet in length. Fans, 5 and 6, mounted inside the cylinders constantly mixed air within. When either normally-closed solenoid valve 3 or 4 was actuated, the "running-average" sample flowed through the intake manifold to the hygrometer as the result of a negative pressure developed by a second (not shown) vacuum pump internal to the hygrometer.

In the field, the orifices of intake hoses, 1 and 2, were placed at desired levels on the vertical instrument tower. (This was immediately adjacent to temperature sensors approximately 40 cm apart.) The Millipore vacuum pump ran continuously so that both sample tanks could provide continuous integrated air samples to the hygrometer. Valves, 3 and 4, were actuated alternately by the input scanner on the recording system. On a given 3 minute recording cycle only one measurement of dewpoint temperature was made. On the succeeding cycle a second measurement was made from the other cylinder. Over a thirty minute period, 10 dewpoint measurements were made, 5 from each cylinder (or tower level). The

average of this set of 5 measurements determined the mean vapor pressure for a given level. Differences in the mean values provided the vapor pressure gradient upon which evaporative flux calculations are based.

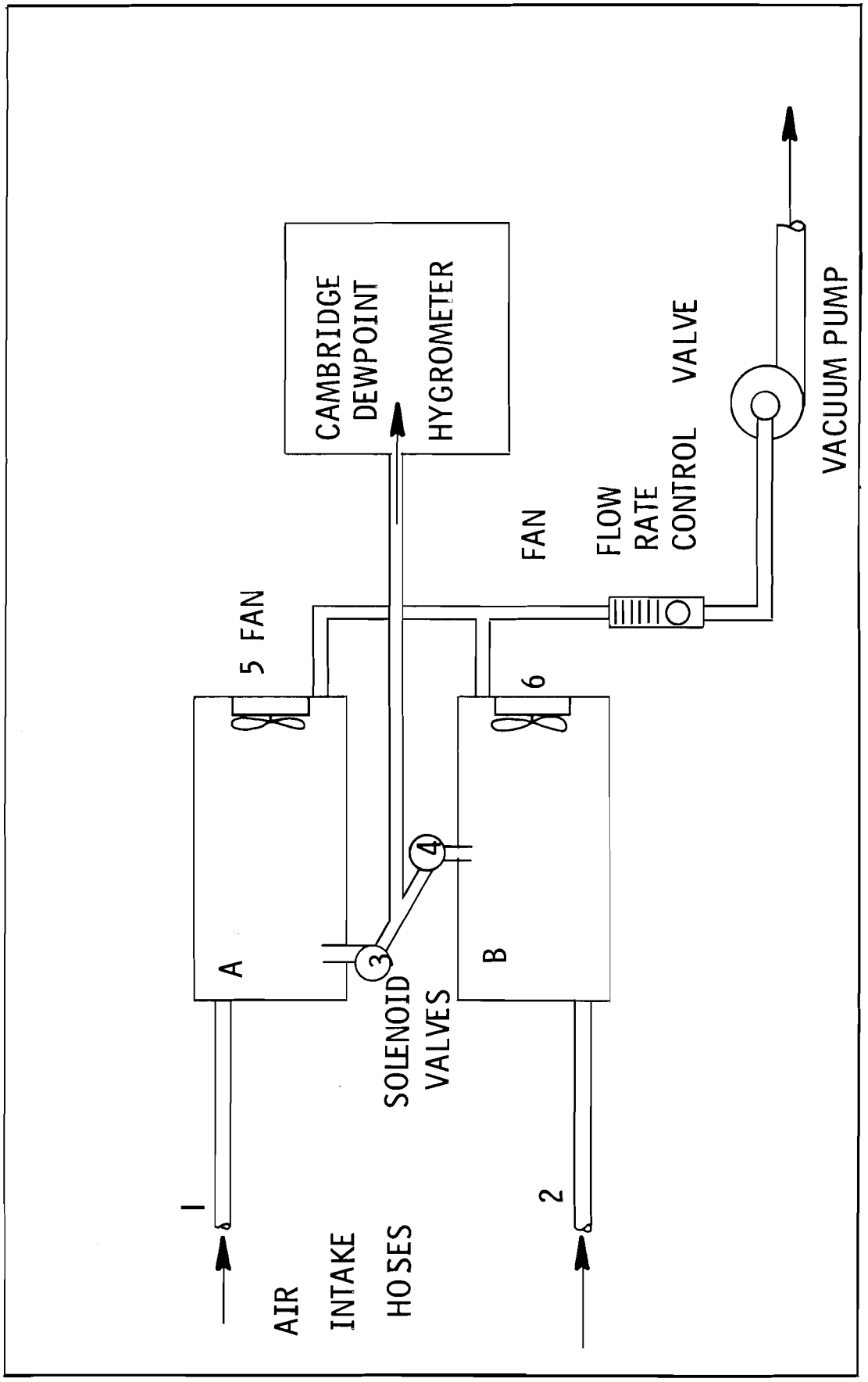

FIGURE 2 SHOP BUILT WATER VAPOR SAMPLING SYSTEM

III. DISCUSSION & CONCLUSIONS

Influence of Energy Budget Components on Hourly Rates of Evapotranspiration

Hourly variations in energy balance components are shown in figures 3-8. Figure 6 for June 4th shows the energy balance on a cloudless day. Centers of symmetry for net radiation and soil heat flux curves occur at 1346 hours, true solar noon at 117° W. On the other five days the diurnal trend is hidden due to the influence of cloud cover.

Details of the clear sky radiation balance are shown in Table 3. Surface albedo was measured by use of a star pyranometer and found to be relatively constant 13.0±1 percent under clear sky conditions (5). Net radiation, R_n, was a linear function (r=0.99) of incoming solar radiation, SWI, and can be expressed as:

$$R_n = 0.113 - 0.749\ SWI \quad (7)$$

where R_n and SWI are given in LY/min.
On cloudy days a similar relationship exists but there is more scatter found in the data ($r \neq 0.99$) due to sampling problems inherent in intermittent cloud cover. R_n can be estimated with reasonable accuracy (±0.03 Lys) using equation 7. This is an advantage since measurements of SWI are more easily obtained.

The close correlation between the magnitude of the soil heat flux, G, and R_n, is shown in Table 3. Since (R_n+G) is the basic source of energy used in evapotranspiration the interaction of these terms is of particular interest.

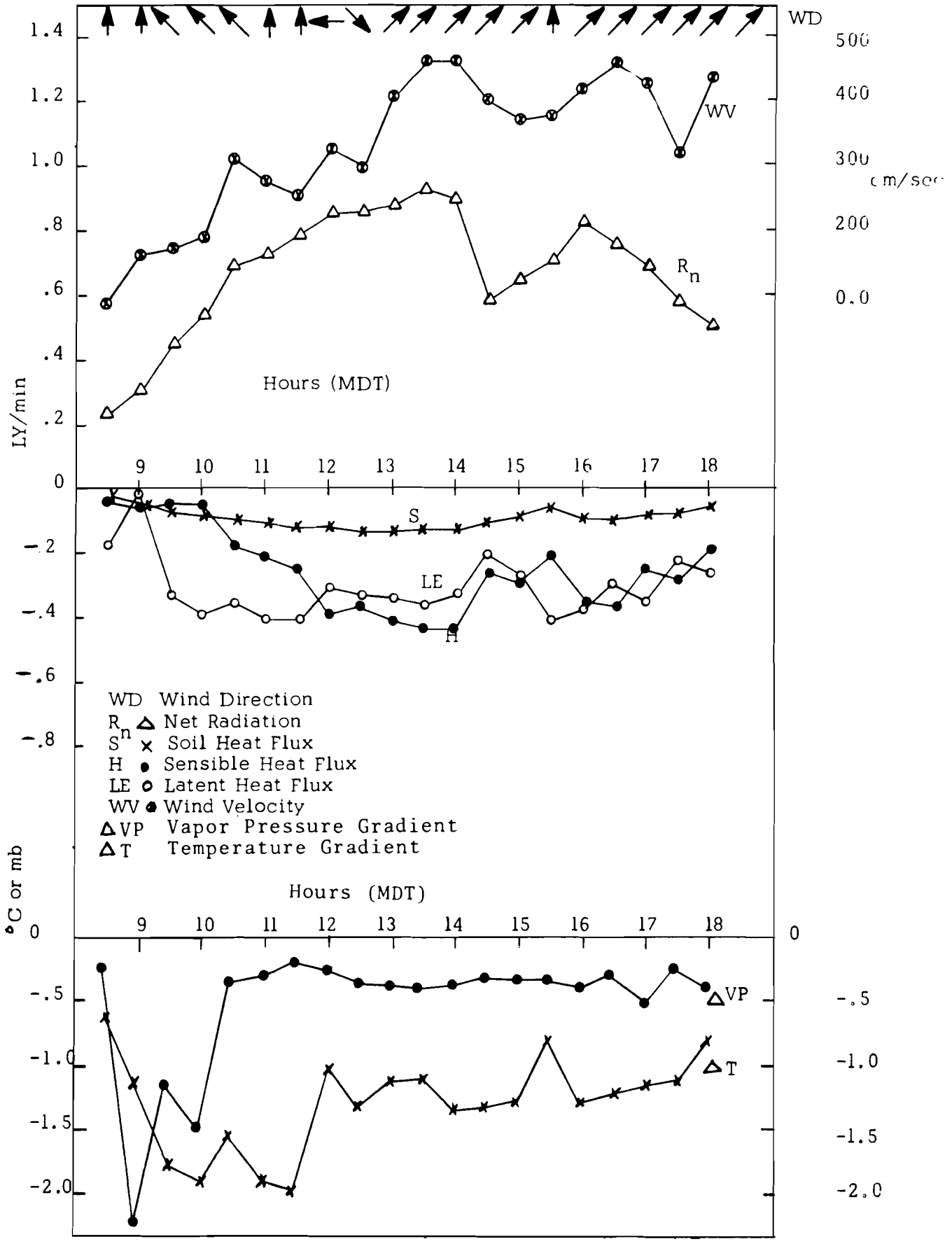

FIGURE 3: Energy Balance at Sheep Creek, May 23, 1969

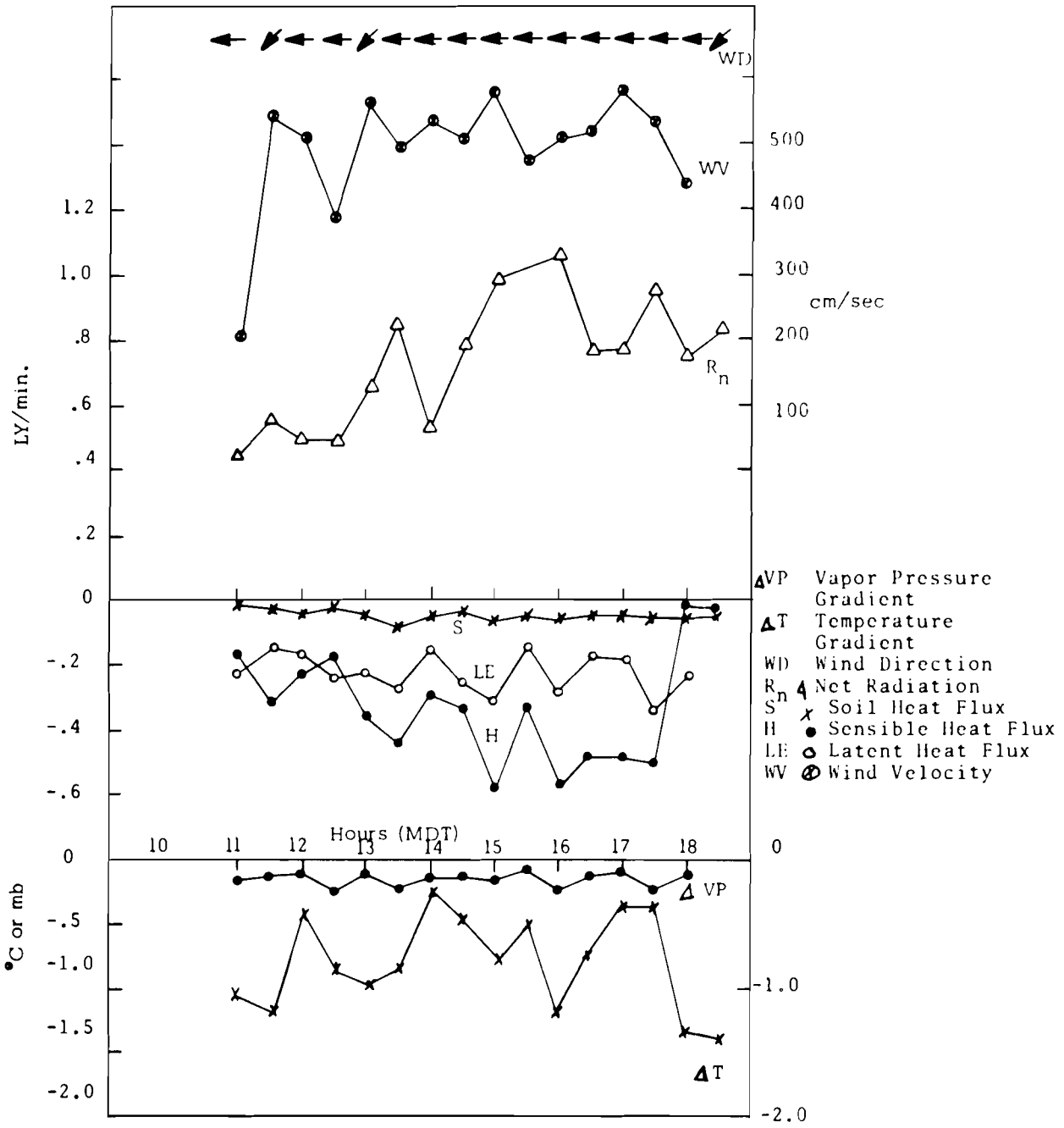

FIGURE 4: Energy Balance at Sheep Creek, May 27, 1969

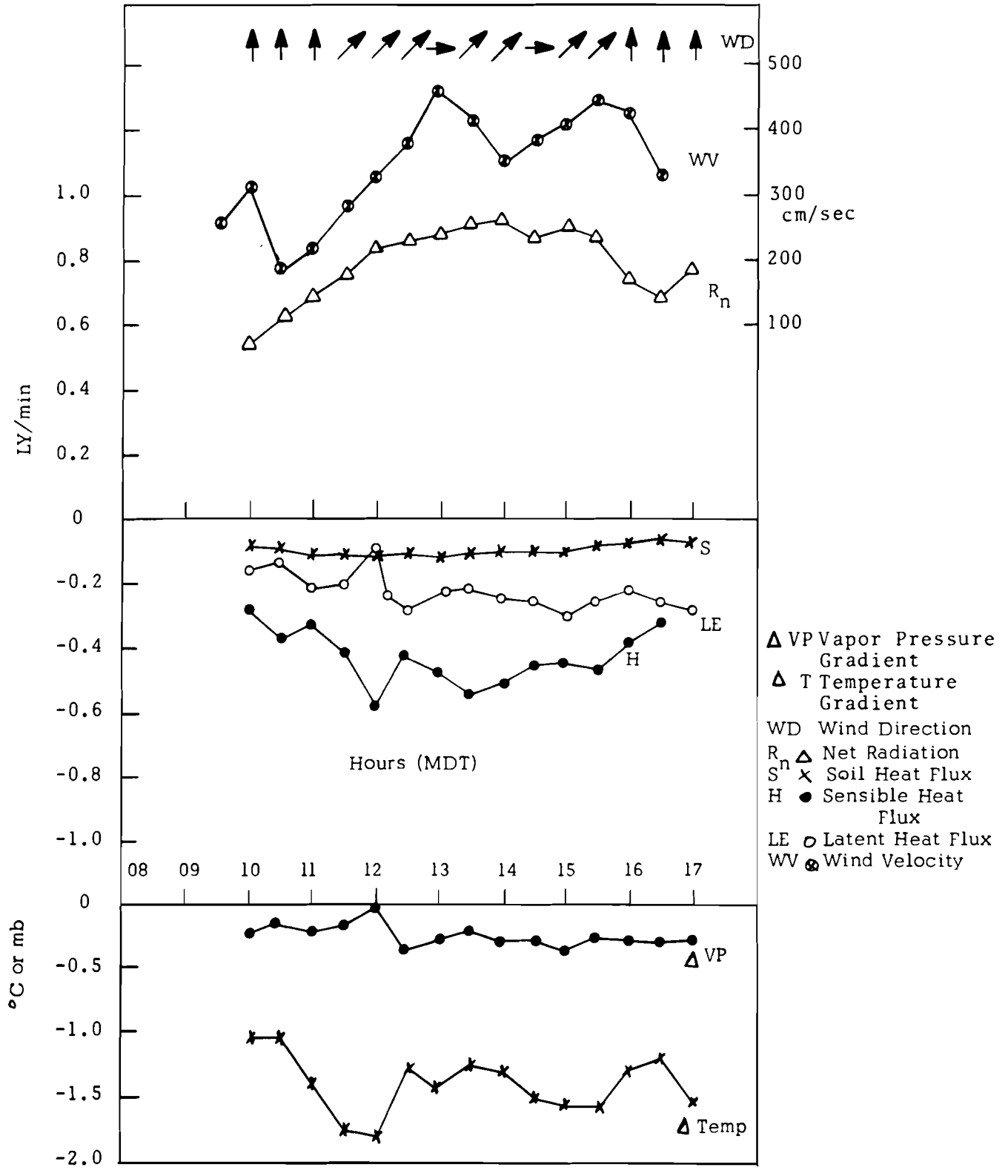

FIGURE 5: Energy Balance at Sheep Creek, May 28, 1969

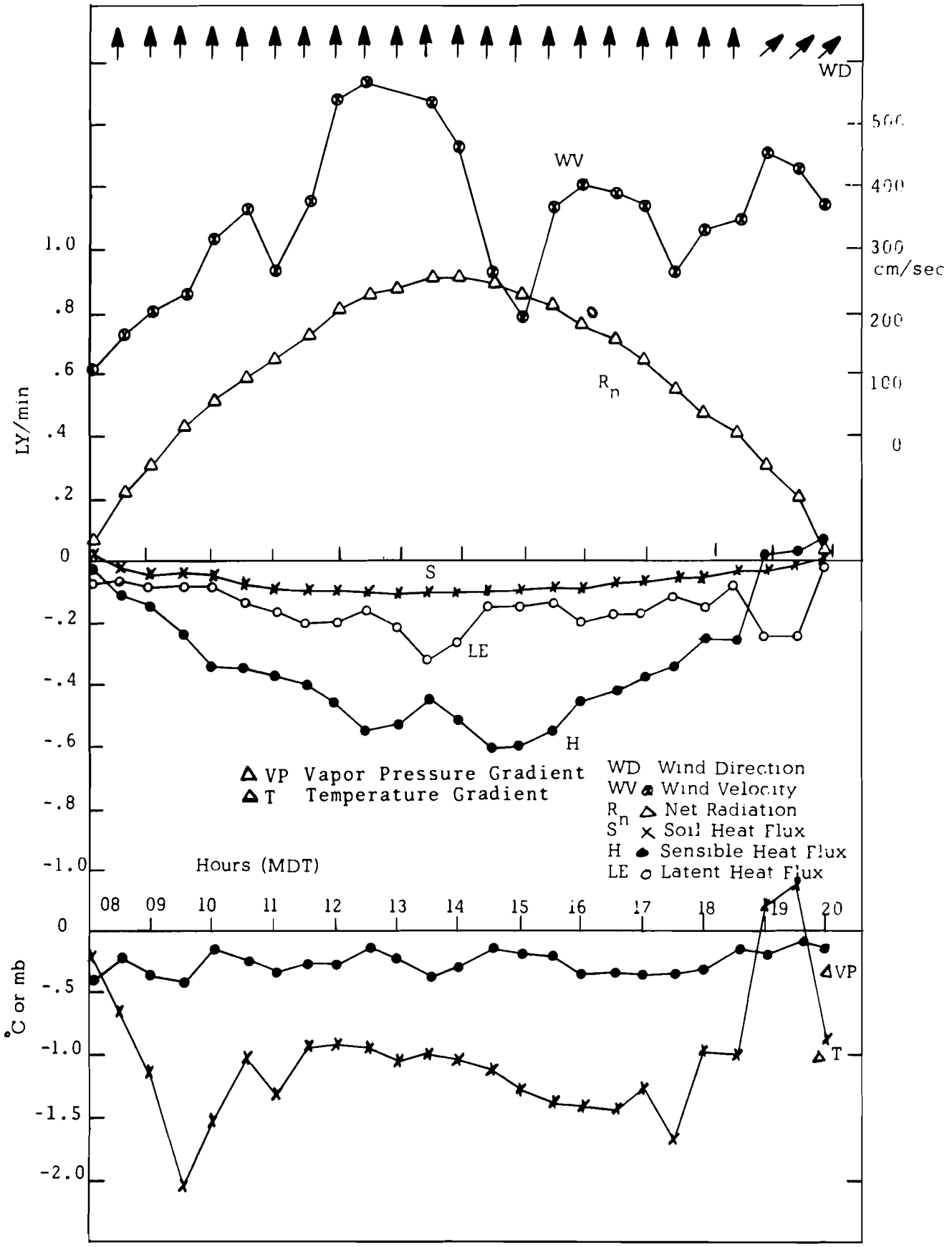

FIGURE 6: Energy Balance at Sheep Creek, June 4, 1969

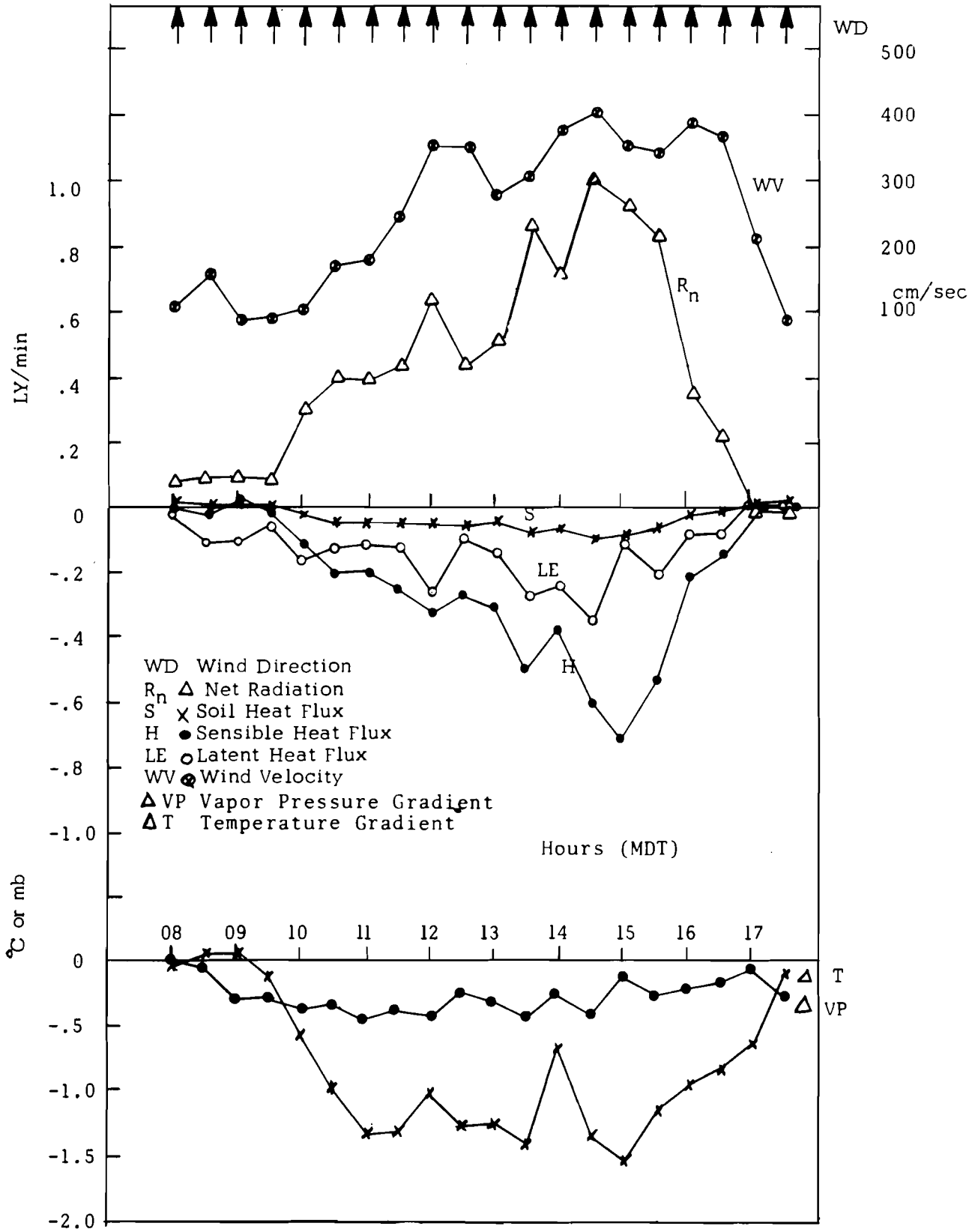

FIGURE 7: Energy Balance at Sheep Creek, June 9, 1969

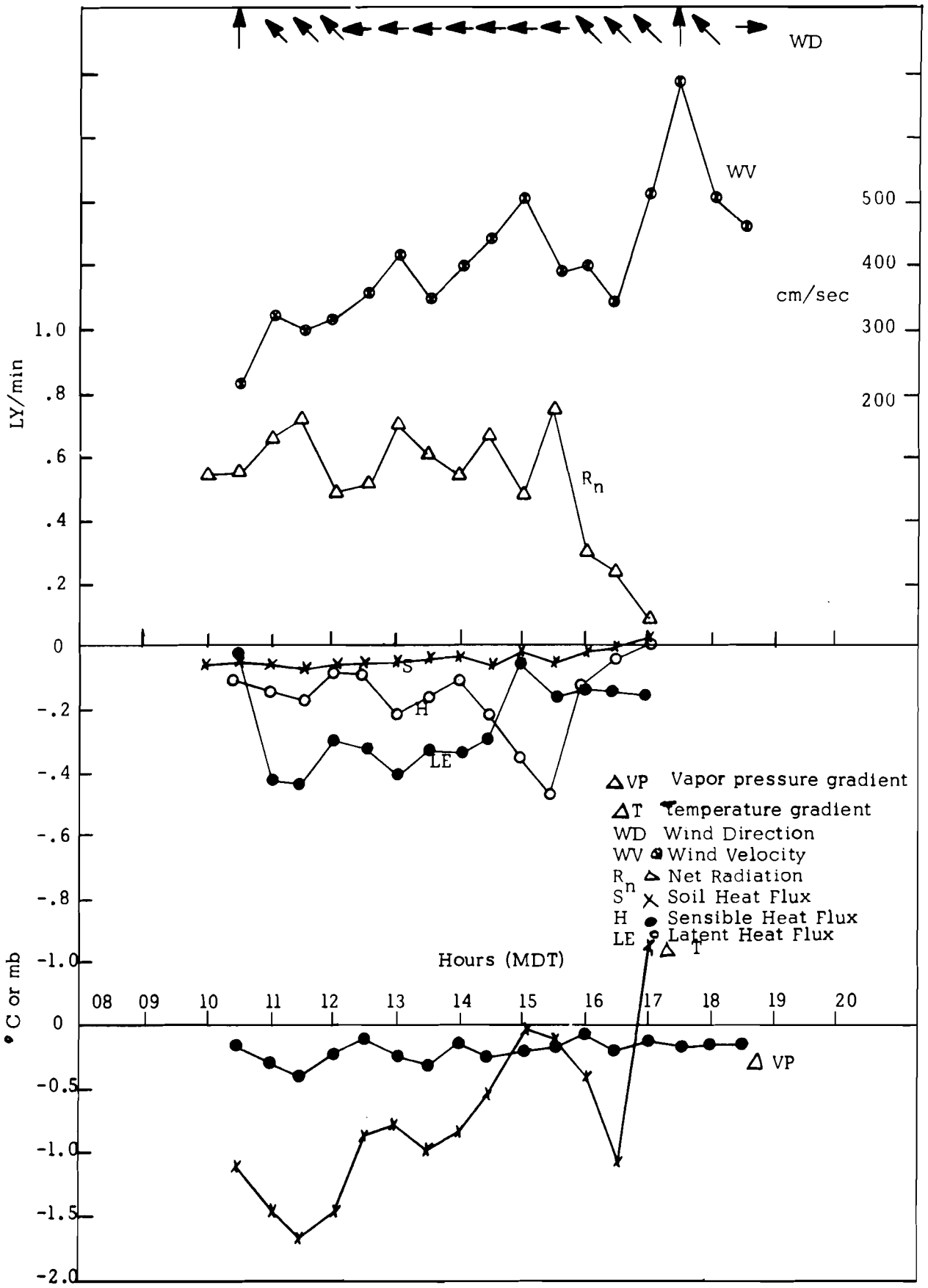

FIGURE 8. Energy Balance at Sheep Creek, June 10, 1969

Time (MDT)	R_N	SWI	SWR	SWN	LWN	G	R_N+G
0800	.07	.29	-.04	.25	-.18	-.00	.07
0830	.23	.42	-.06	.36	-.13	-.02	.21
0900	.33	.54	-.07	.47	-.14	-.04	.29
0930	.44	.68	-.09	.59	-.15	-.06	.38
1000	.54	.81	-.11	.70	-.16	-.07	.47
1030	.63	.93	-.12	.81	-.18	-.08	.55
1100	.66	1.03	-.13	.90	-.24	-.10	.56
1130	.73	1.13	-.15	.98	-.25	-.11	.62
1200	.80	1.21	-.16	1.05	-.25	-.11	.69
1230	.85	1.27	-.17	1.10	-.25	-.11	.74
1300	.88	1.31	-.17	1.14	-.26	-.11	.77
1330	.91	1.34	-.17	1.17	-.26	-.11	.80
1400	.91	1.35	-.18	1.17	-.26	-.10	.81
1430	.89	1.34	-.17	1.17	-.28	-.10	.79
1500	.87	1.31	-.17	1.14	-.27	-.10	.77
1530	.82	1.30	-.17	1.13	-.31	-.10	.72
1600	.78	1.21	-.16	1.05	-.27	-.10	.68
1630	.72	1.14	-.15	.99	-.27	-.09	.63
1700	.65	1.05	-.14	.91	-.26	-.08	.57
1730	.56	.95	-.12	.83	-.27	-.08	.48
1800	.48	.85	-.11	.74	-.26	-.06	.42
1830	.42	.73	-.09	.64	-.22	-.05	.37
1900	.33	.59	-.08	.51	-.18	-.03	.30
9300	.22	.45	-.06	.39	-.17	-.02	.20
2000	.11	.32	-.04	.28	-.17	-.00	.11
2030	.00	.19	-.02	.17	-.17	-.01	-.01

R_N = Net all-wave radiation = SWN + LWN

SWI = Incoming (direct + diffuse) solar radiation

SWR = Reflected solar radiation = 0.BSWI

SWN = SWI + SWR

LWN = R_N - SWN

G = Soil heat flux

Table 3: Radiation Balance for Sheep Creek Study Site, June 4, 1969 (Ly/min.)

Because of spatial variability of soil moisture, soil structure and vegetative cover, the three soil heat flux sensors used provided less accuracy of measurement (on a percentage basis) than did the single measurement of R_n. Soil heat flux was normally less than 15 percent of R_n except when R_n decreased to less than 0.1 Ly/min. In the latter case, measurements of G induced considerable error in $-(R_n+G)$ of equation 6. At these times, estimates of E.T. became unrealistic and had either to be deleted or obtained by interpolation. Fortunately small radiation fluxes occurred primarily at sunrise or sunset when E.T. rates were small. Consequently, such errors were minor. A second type of error is induced in estimates of E.T. when β of equation (6) approaches -1. In this case $\beta+1\rightarrow 0$ and E.T.$\rightarrow \infty$. As suggested by the β in Figure 9, such errors were infrequent in this study. When they did occur, interpolation was used to obtain more realistic E.T. estimates.

Sensible and latent heat flux curves exhibit little symmetry but maximum flux rates appear after solar noon suggesting a time lag of approximately one hour, this is most apparent in Figure 6. An increase in the latent heat flux at 1900 on June 4th was due to a shift in wind direction which resulted in a change from lapse to inversion conditions. This same phenomenon can be observed from 1430 to 1830 on June 10th in Figure 8. When such stable temperature gradients occurred, marked increase in the E.T. rates were indicated as required by Equation 6. Such conditions, however, were infrequent during daylight hours and advective energy had

little influence on total evapotranspiration.

The most significant factor determining variation in the hourly rates of E.T. was the interaction of temperature and vapor pressure gradients. Variation in these gradients about their respective daily means are summarized in Table 4. Daily mean values of the temperature gradient were 1.5 to 4 times larger than the vapor pressure gradient accounting for the magnitude of the Bowen ratios presented later in Table 6. Standard errors for the mean daily temperature gradients were larger than standard errors for the mean vapor pressure gradients on four of the six days tested and approximately equal to standard erros of the mean vapor pressure gradient on the other two days.

Temperature gradients were the more dynamic factor in the Bowen ration and account for most of the variability in hourly values of the ratio plotted in Figure 9. This temporal variability is due to the relatively small volumetric heat capacity of air and the rapid cooling and heating of the surface-air-layer in response to variation of the radiation flux and wind speed. Correlation coefficients were obtained between hourly temperature gradients and mean wind speed at 250 cm. These coefficients, presented in Table 5 in descending order, range from -0.86 to -0.09 on June 10th and 4th respectively. The linear relationship between gradients declines as daily net radiation increases.

This suggests wind speed has the greater influence in determining temperature gradients under overcast conditions.

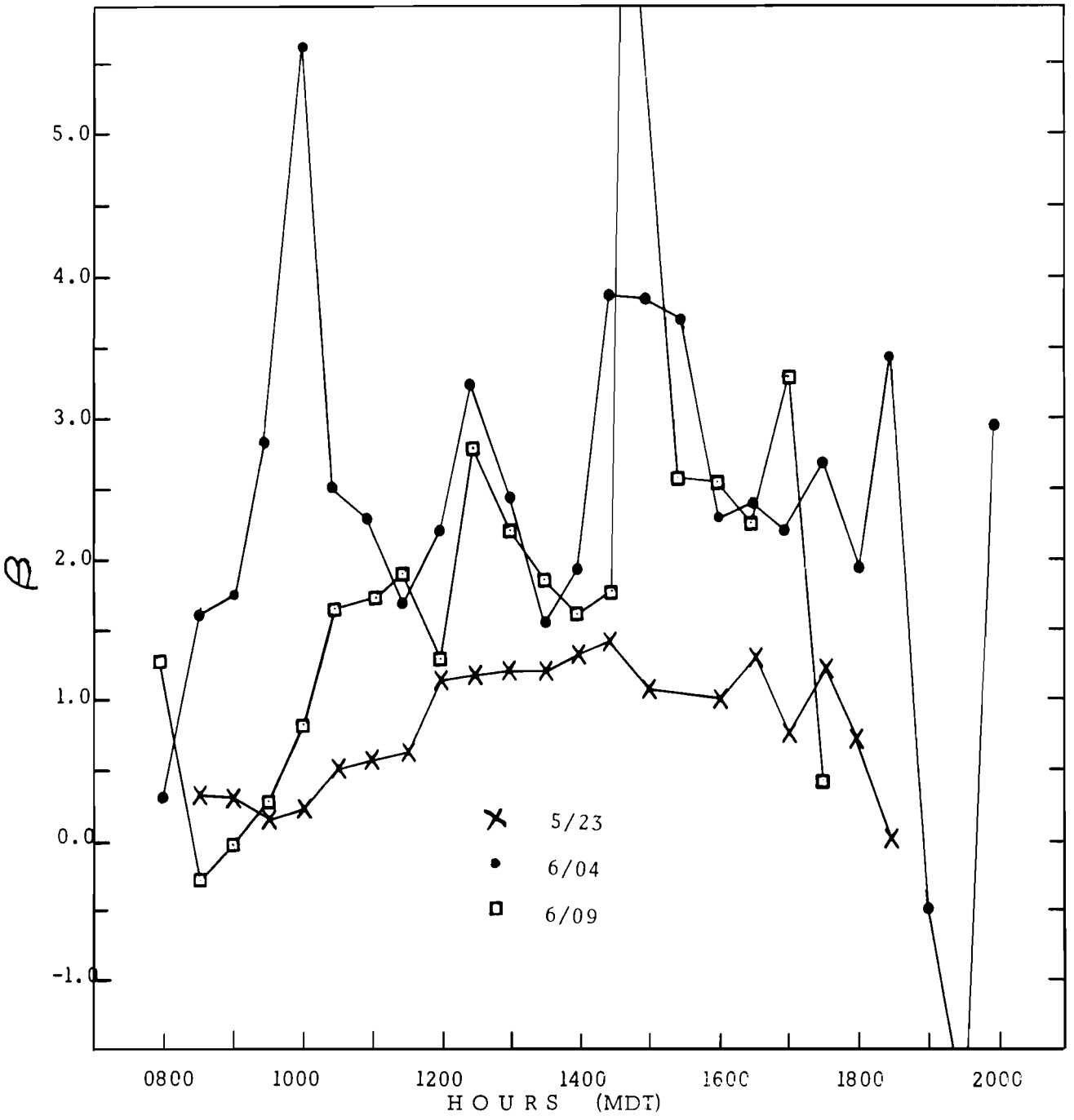

FIGURE 9: Diurnal variability of the Bowen Ratio

Day	$\Delta\bar{e}$(mb)	Standard Error	Coeff. of Variation	$\Delta\bar{T}$(°C)	Standard Error	Coeff. of Variation	Δz (cm)
5/23/69 0830-1800	-.55	.54	-.99	-1.28	.45	-.35	80
5/27/69 1000-1700	-.18	.05	-.29	- .79	.34	-.43	
5/28/69 1000-1700	-.25	.07	-.29	-1.42	.22	-.15	
6/04/69 0830-1730	-.26	.08	-.31	-1.03	.53	-.51	40
6/09/69 0800-1730	-.16	.55	-3.31	- .84	.52	-.62	
6/10/69 1030-1830	-.22	.06	-.29	- .47	.95	-2.01	

Table 4: Standard Errors and Coefficients of Variation for Average Daily Vapor Pressure and Temperature Gradients Measured at Sheep Creek

Day	Time	Total Daily R_n	Correlation Coefficient ($r\Delta T:V$)	Mean Daily Wind Speed (cm/sec)
6/10/69	1030-1830	215.3	-.86	382
6/09/69	0800-1730	257.9	-.67	269
5/27/69	1000-1700	316.2	-.34	485
5/28/69	1000-1700	349.5	-.25	350
5/23/69	1000-1700	392.1	-.21	228
6/04/69	0800-2030	444.8	-.09	306

Table 5: Dependency of Temperature Gradient, Δ T, on Wind Speed, V, and Total Daily Net Radiation

Under clear skies, when the radiant heat flux is greater, surface energy supply is probably the more dominant factor. These hourly variations in the Bowen ratio as discussed above appear to be the dominant factor in inducing variation hourly estimates of E.T. as calculated from equation 6.

Daily Evapotranspiration Losses

The energy balance during daylight hours is summarized in Table 6 for the Sheep Creek area. It should be noted in Table 6 that the energy balance data is summarized for different periods each day (due to instrumental difficulties) and is not comparable on an absolute basis. The differences in net radiation, for example, are a function of both cloud cover and the time of the daily measurement period. The same statement applies to total E.T. listed in column 5. Note, however, that the absolute E.T. losses for May 28, June 4, and 9, -0.07, -0.08, and -0.06 respectively compare well with the average daily evaporative loss, -0.07", calculated on the basis of soil moisture data presented in Table 1. While no absolute standard of comparison is available, this agreement suggests that E.T. estimates obtained are of the correct order of magnitude. To facilitate comparison of the energy balance components between days and to examine trends during the period of observation, the flux components have been expressed as a percent of net radiation in column 7, 8, and 9 of Table 6. Bowen ratios computed on the basis of daily totals of H and LE are also listed. Note that the soil heat flux, G, is relatively constant, 11-15 percent on each of the six days. The bulk of the radiative flux, 85-89 percent, is partitioned into H and LE as shown in column 7 and 8.

Changes in the Bowen ratio during the period of observation, column 6, show the influence of precipitation and

Day/Time	Net Radiation (Rn) Ly	Soil Heat Flux (G) Ly	Sensible Heat Flux (H) Ly	Latent Energy (LE) Ly	Evapo-trans piration in.	H/LE (β)	LE/Rn %	H/Rn %	G/Rn %
Column	1	2	3	4	5	6	7	8	9
5/23/69 0830-1800	392.08	-59.02	-154.15	-179.02	-0.12	0.86	-46	-39	-15
5/27/69 1000-1700	316.24	-40.04	-164.67	-110.53	-0.074	1.49	-35	-52	-13
5/28/69 1000-1700	349.50	-44.32	-197.13	-108.05	-0.07	1.82	-31	-56	-13
6/04/69 0800-2030	444.82	-59.23	-261.46	-124.13	-0.08	2.10	-28	-59	-13
6/09/69 0800-1730	257.91	-37.03	-137.83	- 83.01	-0.06	1.66	-32	-53	-14
6/10/69 1030-1830	215.30	-23.85	-120.37	- 71.07	- .05	1.69	-33	-56	-11

Table 6: Energy Balance and Evapotranspiration Data, Sheep Creek Site May-June, 1969

subsequent changes in soil moisture on evapotranspiration. During the period from May 23 to June 4, the Bowen ratio was increasing suggesting a decrease in the evapotranspiration flux or a general drying trend in the soil as indicated by the soil moisture profiles. During this period only traces of precipitation were recorded. During the period from June 5 to June 10, 0.81" of precipitation were recorded. The Bowen ratio subsequently decreased on June 9 and 10 indicating the increased partition of energy into the latent flux in response to the increased soil moisture availability. The same explanation is appropriate to changes in the ratios LE/R_n and H/R_n in columns 7 and 8 of Table 6.

Close correlation between R_n and LE for well watered surfaces has frequently appeared in the literature. For example, data of Frankenberger in Fowler (1964), for Quickborn, yielded a regression equation (units in Ly/day)

$$LE=0.664\ R_n + 18.5 \qquad (8a)$$

with a correlation coefficient, r value, of 0.96. Similarly, Pruitt (1964) reported for rye grass:

$$LE=0.98\ R_n + 0.05 \qquad (8b)$$

with an r value of 0.96.

For low sagebrush, where water was limiting, a similar regression of LE on R_n values from Table 6 yields:

$$LE= 0.342\ R_n + 0.14 \qquad (9)$$

with an r value of 0.77 and standard error of estimate of 22 Ly per day or approximately 0.02" per day, 20-30 percent. This latter prediction equation, valid only for similar con-

ditions of soil moisture, etc., does not have the high degree of linear correlation of 8a and 8b. Inspection of the plotted data (Figure 10) shows the smaller correlation coeffcient results primarily from deviations about the regression line which occurred on May 23 and June 4, days when the mean daily Bowen ratio exhibited minimum and maximum values and soil moisture extremes most probably existed. While most of the proceeding discussion follows implicitly from energy balance-Bowen ratio methodology, it should be noted that for the rangeland site studied, R_n essentially placed an upper limit on maximum E.T. losses due to the minor role of advected energy, i.e. $LE/R_n < 1.0$. This is in contrast to the situation for many irrigated crops where frequently the ratio $LE/R_n \geq 1.0$ due to the addition of advected heat. Finally, it is important to stress that while R_n placed an upper limit on E.T. from the Sheep Creek site, actual E.T. losses were strongly modulated by soil moisture availability as reflected in the magnitude of the Bowen ratio.

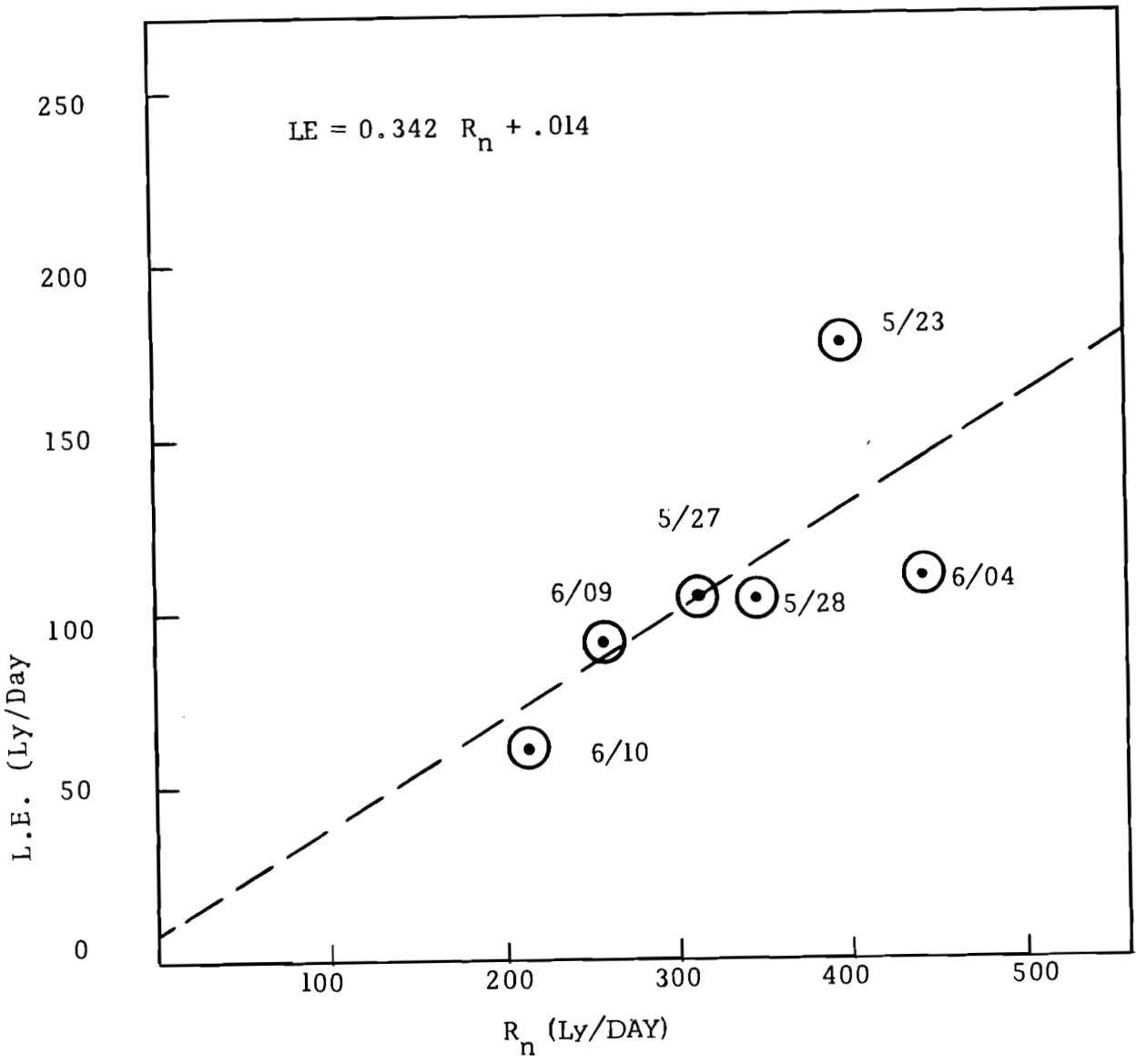

FIGURE 10: Dependence of laten energy flux, L.E., on net radiation flux, R_n, for days shown in Table 6. Note that some deviation about the regression line is due to the difference in measurement periods indicated in Table 6.

IV. SUMMARY

1. Evaptranspiration was measure from low sagebrush covered range during the spring of 1969. Rates of E.T. on an average daily basis were estimated using the energy balance-Bowen ratio procedure. Average daily E.T. rates ranged from 0.05" to 0.12" under differing conditions of soil moisture and radiant energy supply. Latent energy flux accounted for 28 - 46 percent of net radiation during daylight hours. Soil heat flux was a relatively constant, 11-15, percent of net radiation. On all but one of the 6 days of observation, more energy was partitioned into sensible heat than latent heat indicating moisture availability, not energy availability, was the limiting factor during the spring period. This was true even though significant amounts of precipitation and overcast conditioning occurred during the period of measurement.

2. Evaporation in units of Ly/day can be estimated for similar low sagebrush range and soil moisture conditions (approx. 33% by vol.) by use of equation (9) $LE = 0.342 R_n + 0.14$. Such estimates should be within $\pm$30 percent for a given day and better accuracy should be obtained when daily totals are used to obtain weekly averages.

3. Advection of heat energy did not add to evaporative loss during the period of observation.

4. Albedo of the vegetated surface was 0.13 and varied insignificantly as a function of solar angle.

5. Net radiation can be predicted accurately from measurements of insolation due to the constant surface albedo.

Net radiation can be predicted by equation (7) $R_n = 0.113 - 0.749$ SWI.

6. Hourly variations in E.T. rates are determined primarily by changes in the Bowen ratio. The magnitude of the ratio is determined by both vapor pressure and temperature gradients, the latter being the more variable. Variation in temperature gradients are correlated with mean wind velocity during overcast conditions but are primarily determined by the net radiation flux during clear skies.

References

(1) Waggoner, P.E. et. al. 1965. Agricultural Meteorology, Meteorological Monograph No. 28, Vol.6, American Meteorological Society.

(2) Fritschen, L.J. 1965. Accuracy of Evapotranspiration Determinations by the Bowen Ratio Method. Bulletin of the Inter. Society of Scientific Hydrology Vol. X, No. 2.

(3) Tanner, C.B. 1960. Energy Balance Approach to Evapotanspiration from Crops. Proceedings, Soil Science Society of America Vol. 24. p. 1-9.

(4) Bowen, I.S. 1926. The Ratio of Heat Losses by Conduction and Evaporation from any Water Surface, Physics Review, Vol. 27. p. 779-787.

(5) Dirmhirn, Inge. 1969. Personal Communication.

(6) Fowler, W.B. 1964. The Energy Budget and Its Use in Estimating Evapotranspiration Proceedings, Society of American Foresters, Denver, Colorado.

(7) Pruitt, W.O. 1964. Cyclic Relations Between Evapotranspiration and Radiation. Transactions of the ASAE. Vol. 7, No. 3. p. 271-275.

APPENDIX

Integrated Circuit- Pulse Counters

by

Douglas Denny and Joe Thomas[1]

The basic function of this counter circuit is to count pulses produced by an anemometer and place them in a format which can be printed on command by a teletypewriter.

A block diagram for the counting system is shown below.

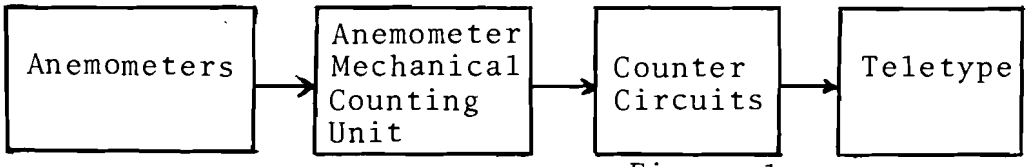

Figure 1

Anemometers and the anemometer mechanical counting units are of commercial design manufactured by C.W. Thornwaite Associates. The teletype is a commercial unit manufactured by Teletype Corporation. Anemometer data is one of several types of data fed to the teletype unit for recording. The counter circuit was designed to be used for several counting applications; it was to be specifically adaptable to counting and storing in the anenometer.

The counter circuit shematic is shown in Figure 2. It is constructed entirely of solid state components whose active parts consist of Motorola RTL integrated circuits and transistors. A block diagram illustrating the various functions of the counter circuit is shown in Figure 3.

---

[1] The authors are respectively, student and Assistant Professor of Electrical Engineering, University of Idaho, Moscow.

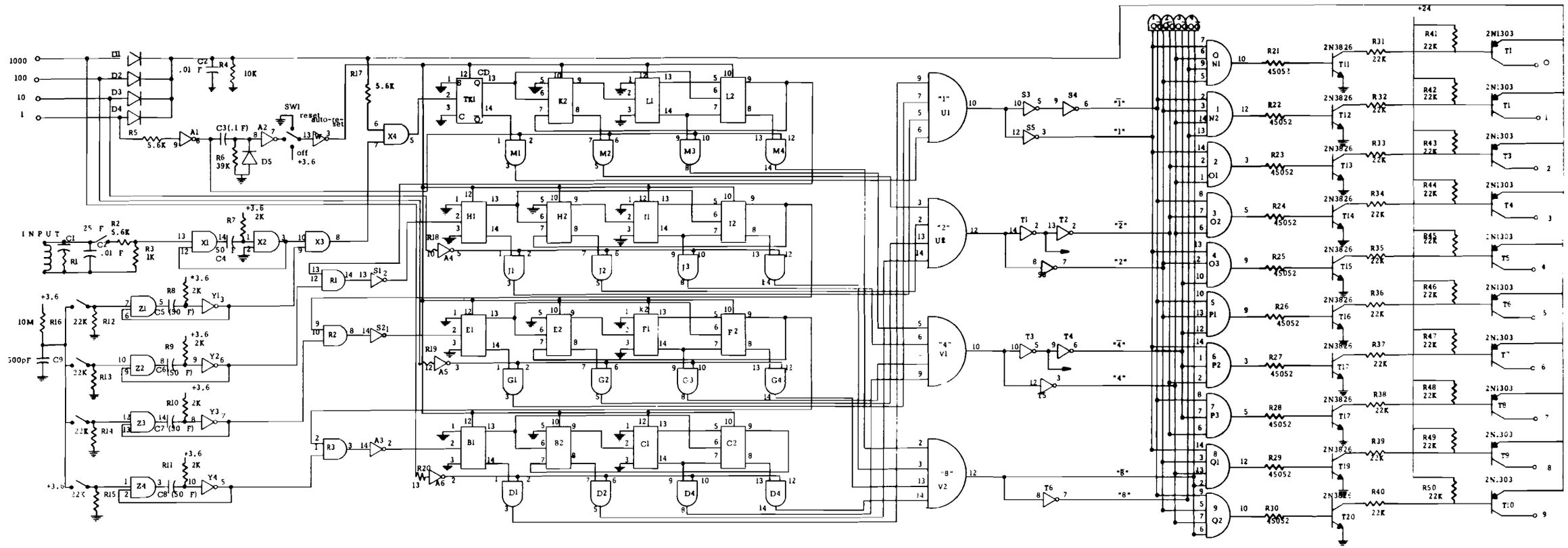

FIGURE 2: Counter Schematic Diagram

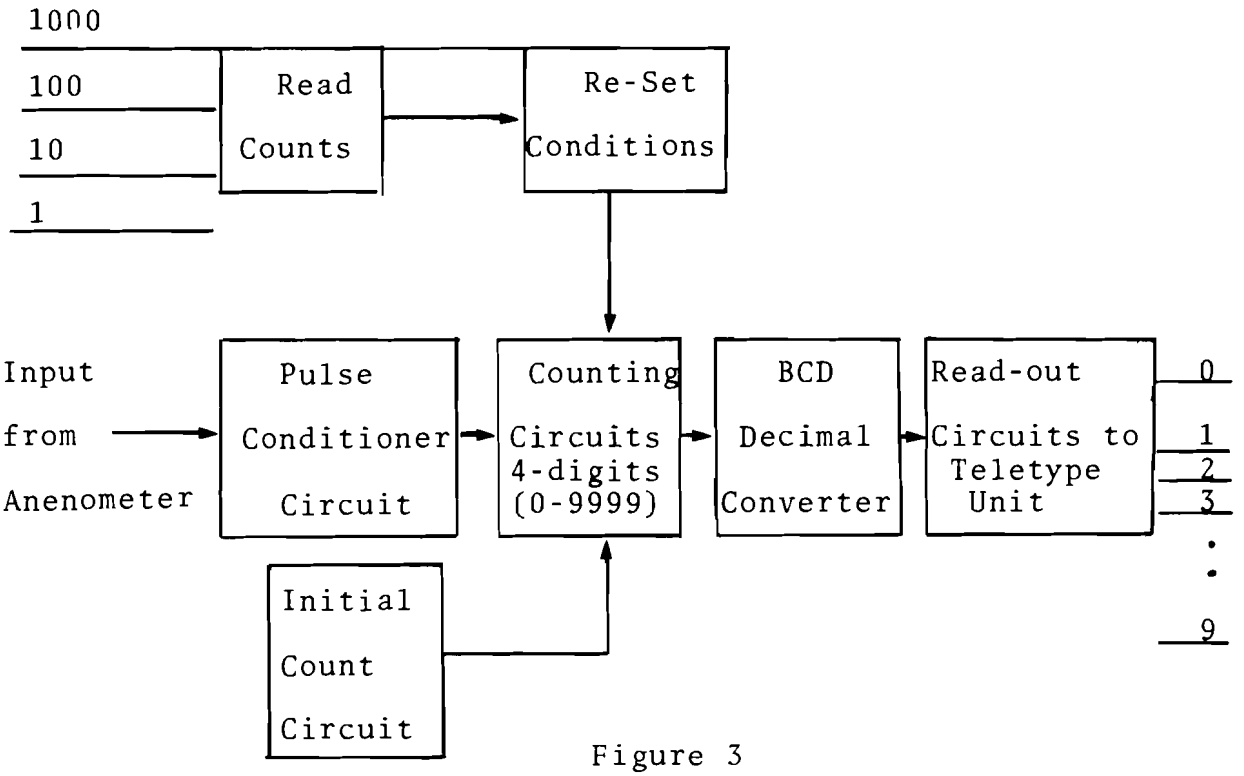

Figure 3

The input to the circuit is fed into the pulse conditioner circuit. The latter network consists of L_1, C_1, C_2, R_1, R_2, and R_3 on the schematic. Output of R_3 is fed into the input of gate X (a monostable multivibrator) where it is formed into a pulse 50 milliseconds in duration. The function of the network consisting of L_1, C_1, C_2, R_1, R_2 and R_3 is to eliminate noise picked up on the input line.

The monostable multivibrator consists of two gate units marked X_1 and X_2. The output from this multivibrator is fed into the counter circuits directly through another gate X_3. X_3 is an "NOR" gate which allows the initial value units count to be fed to the units counter.

The units counter consists of circuits marked K_1, K_2, L_1, and L_2. Each of these units (K and L consists of two J-K

flip-flops interconnected to provide a count to 10 circuit. When 10 counts have been received, the circuit automatically feeds a pulse to the 10's counter and resets itself. The circuit is a quadruple, two-input gate used to read the Binary Coded Decimal (BCD) information on the units counter.

The tens counter consists of flip-flops H and I connected as a count by 10 circuit. The BCD information is read from these circuits on gates J. The units count is fed into the circuit through the NOR gate R_1 as is the initial value count for the tens counter generated by the switch on Z_2 and Y_2.

The hundreds counter consists of flip-flops E and F with the BCD information gated out of this decade counter through gate G. Output of the 10's counter is fed into the circuit through gate R_2. The initial value is fed into the circuit through gates R_2, Y_3, and Z_3.

The same reasoning applied to the thousands counter consisting of flip-flops B and C with the information being sent through gate D.

After the counter has received pulses from the anemometer for an externally prescribed amount of time, read pulses are fed into the circuit through the read inputs marked 1000, 100, 10, 1 on the schematic. The thousands digit is read first, followed in sequence by the 100, 10, and units. After reading the units count the counters can either be automatically reset or can accumulate additional pulses depending on the position of SW1. With SW1 in the center position the counters will be automatically reset after the read units

command pulse from the teletype. With SW1 in the upper position (arm connected to +3.6V) the counter will accumulate pulses with SW1 in the ground position the counters are manually reset.

Gates U_1, U_2, V_1, and V_2 are used to read information from the counters. The BCD "1" count is read in U_1, the "2" is read in U_2, the "4" is read in V_1, and the "8" is read in V_2. When the read 1000 number pulse is applied to the input the thousands counter is interrogated and the number of 1000's count stored in the counter at that time is fed out in BCD form to U_1,U_2, V_1, and V_2. This is decoded in the BCD to decimal decoder consisting of gates N, O, P, and Q. Decimal information from these gates is fed to the transistors T11 - T20 and T1 - T10. The decimal 0 is fed out on the collector of T1 and the numbers are sequenced such that the decimal 9 is fed out on the collector of T10.

After 1000 counts are read, a signal is received by the 100's input which then interrogates the hundreds counter. This BCD count is again gated out from the information stored in the flip-flops making the 100's counter. This BCD information again goes to gates U and V where it is encoded into decimal form and read out through the output transistors.

The tens counter and the units counter are interrogated in a similar manner.

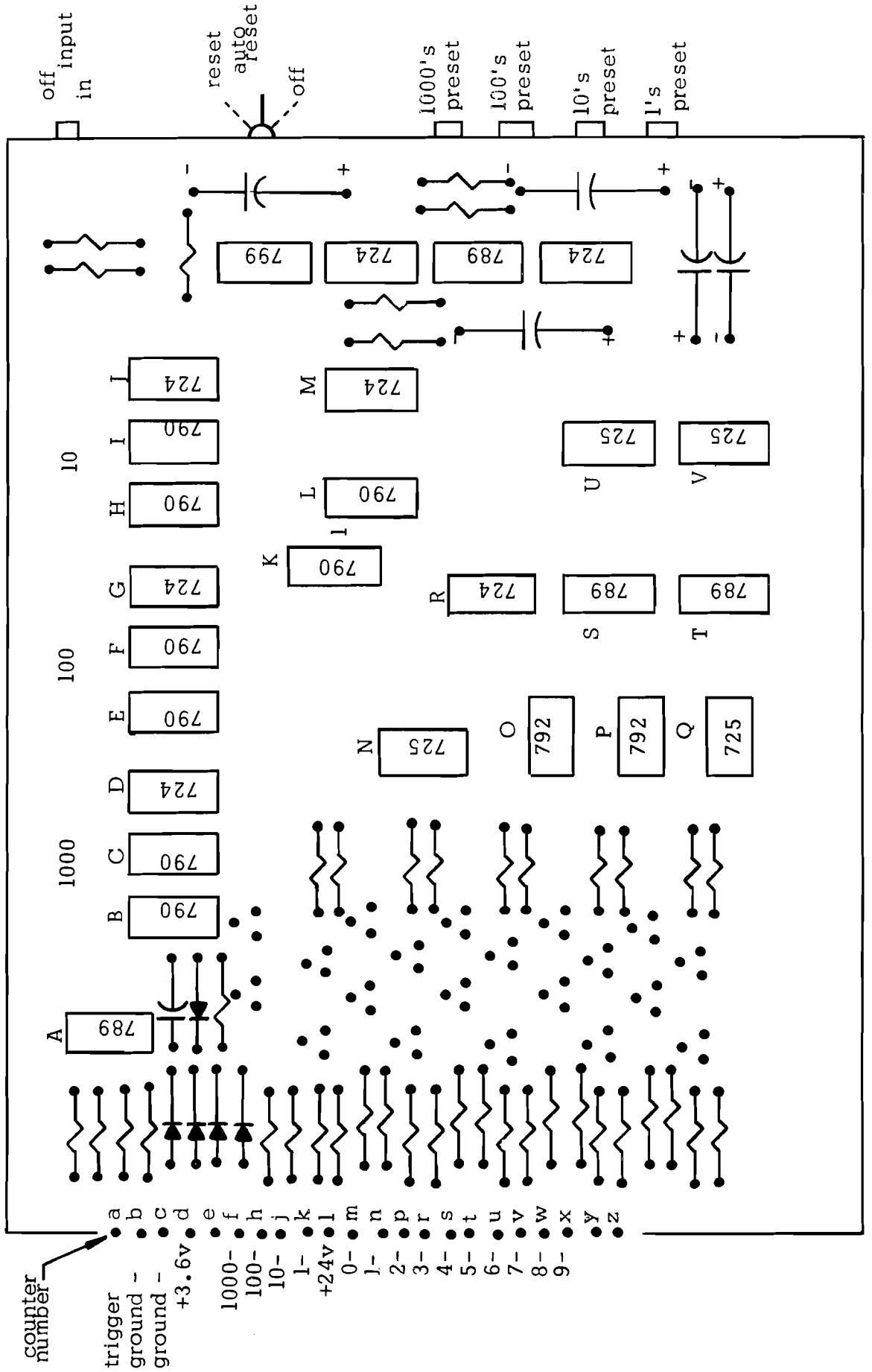

FIGURE 4: Front View of Counter Circuit Board showing position of I.C. components

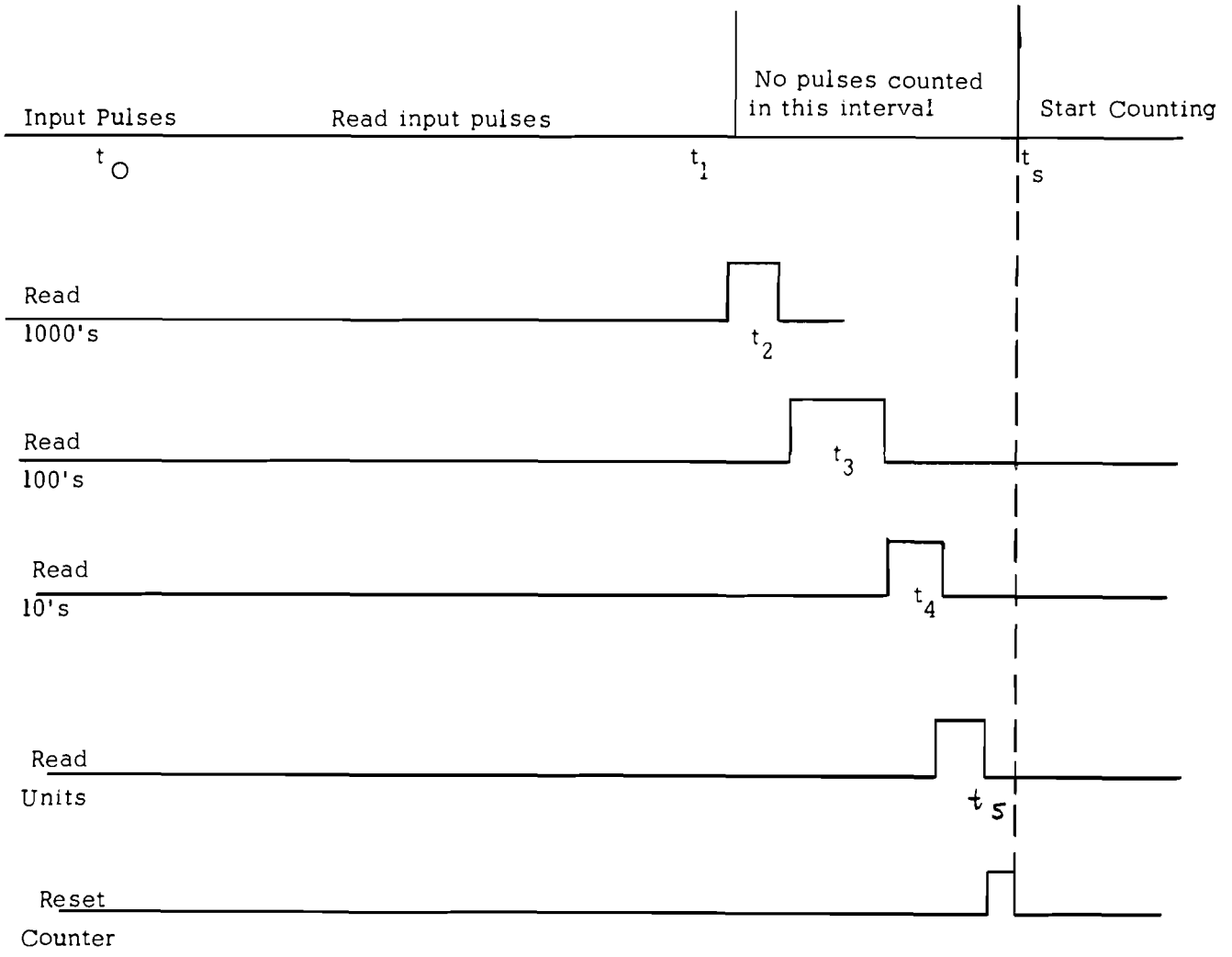

FIGURE 5: Time Sequence for counting process

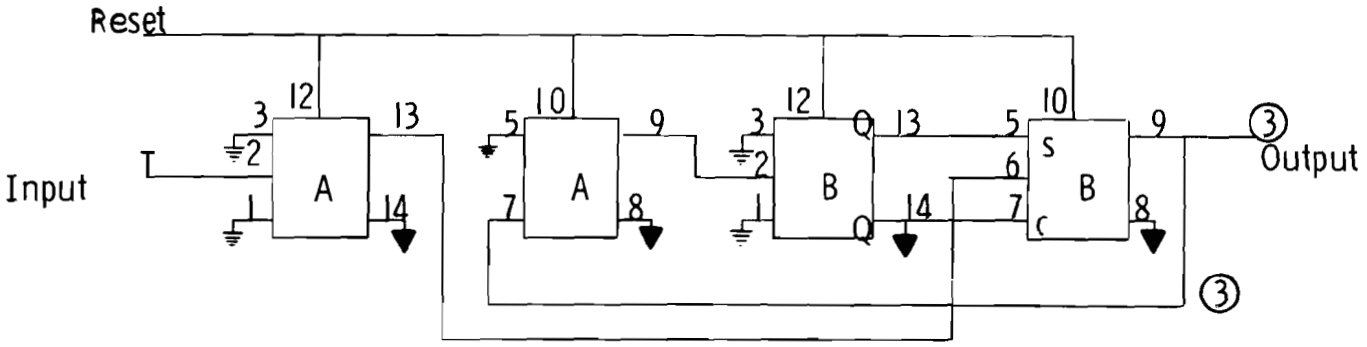

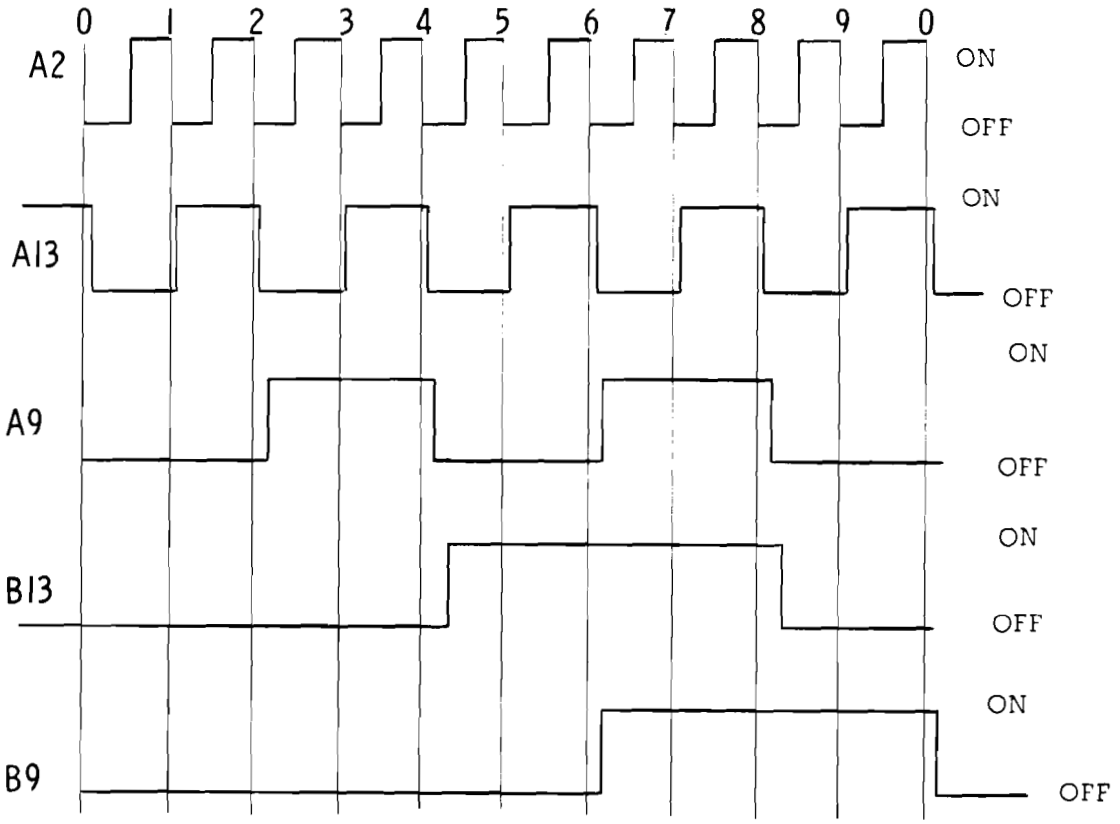

FIGURE 6: Typical count-to ten circuit with reference points and pulse condition, "on" or "off" for counts 0 to 9.

Parts List for Counter Circuit

Capacitors

C1-

C2 - 0.01 f50V

C3-

C4 - 50 f 10V

C5 - 50 f 10V

C6 - 50 f 10V

C7 - 50 f 10V

C8 - 50 f 10V

C9 - 500pf 10V

Resistors: Note: all resistors are 1/4W, 10% unless otherwise noted.

R1-

R2 - 5.6K

R3 - 1K

R4 - 5K

R5 - 560

R6-

R7 - 2K

R8 - 2K

R9 - 2K

R10 - 2K

R11 - 2K

R12 - 22K

R13 - 22K

R14 - 22K

R15 - 22k

R16 - 10 meg.

R17-

R18 - 560

R19 - 560

R20 - 560

R21 - 450

R22 - 450

R23 - 450

R24 - 450

R25 - 450

R26 - 450

R27 - 450

R28 - 450

R29 - 450

R30 - 450

R31 - R50 - 22k

Diodes:

D1

D2

D3 any small signal silicon diold will work here

D4

D5

Transistors

T1 - T10 - 2N1303

T11 - T20 - 2N3826

Integrated Circuits - all are Motorola RTL circuits

A - MC789P

Integrated Circuits (cont.)

B - MC790P

C - MC790P

D - MC724P

E - MC790P

F - MC790P

G - MC 724P

H - MC790P

I - MC790P

J - MC724P

K - MC790P

L - MC790P

M - MC724P

N - MC725P

O - MC 792P

P - MC792P

Q - MC725P

R - MC724P

S - MC789P

T - MC789P

U - MC725P

V - MC725P

W - MC799P

X - MC789P

Y - MC789P

Z - MC724P